

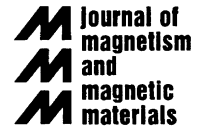


ELSEVIER

Available online at www.sciencedirect.com

SCIENCE @ DIRECT®

Journal of Magnetism and Magnetic Materials 256 (2003) 100–105



www.elsevier.com/locate/jmmm

Magnetic studies in Fe/Zn multilayers

M.A. Morales^{a,*}, H. Lassri^b, H.D. Fonseca Filho^a, A.M. Rossi^a,
E. Baggio-Saitovitch^a

^a Centro Brasileiro de Pesquisas Físicas, CME, Rua Dr. Xavier Sigaud 150, 22290-180 Rio de Janeiro, RJ, Brazil

^b Laboratoire de Physique des Matériaux et de Micro-électronique, Faculté des Sciences Ain Chock, Université Hassan II, B.P. 5366, Route d'El Jadida, Km-8, Casablanca, Morocco

Received 24 July 2001; received in revised form 15 May 2002

Abstract

The structural and magnetic properties of Fe/Zn films prepared by thermal evaporation have been studied by means of X-ray diffraction, vibrating-sample magnetometry and ferromagnetic resonance (FMR). For Fe layer thickness smaller than 20 Å the saturation magnetization decreases with decreasing Fe thickness, which is an indication of the island growth of Zn and Fe–Zn interdiffusion at the layer interfaces. The effective field magnetization $4\pi M_{\text{eff}}$ of the Fe/Zn multilayers was determined from the FMR data in a rotating external magnetic field. The interface anisotropy constant of the Fe/Zn multilayers, K_S , is found to be 1.0 erg/cm² at 300 K. This indicates the presence of a large perpendicular interface anisotropy and this may suggest that the largest part of K_S originates from lattice misfit strain. © 2002 Elsevier Science B.V. All rights reserved.

PACS: 75.70

Keywords: Fe; Zn; Multilayers; Ferromagnetic resonance

1. Introduction

Magnetic multilayers are interesting both from fundamental and applied points of view and are being actively investigated by several laboratories. The properties of these materials are mostly governed by the surface properties and hence the interface plays an important role. The investigation of low-dimensional magnetic behavior in metallic ultrathin films has greatly profited from

molecular beam epitaxy (MBE) techniques. For example, the discovery of coupled magnetic behavior between bilayer components in various magnetic multilayer systems [1–4] has led to an increased interest in two-dimensional (2D) systems.

It has been reported that the magnetization of several Fe multilayer films decreases as the Fe layers become thinner [5–7]. As possible reasons one can mention, (1) the unique properties of thinner films, (2) a change in crystal structure, and (3) a change in the electronic state by interaction between Fe and the substrate atoms, although more detailed work is required for clarification.

*Corresponding author. Tel.: +21-2586-7150; fax: +21-2586-7540.

E-mail address: morales@cbpf.br (M.A. Morales).

It is well known that thin films of low melting point metals such as Pb crystallize with an island structure [7–9], melting point of Pb is 600 K. Such a characteristic is useful to investigate the effects of nonmagnetic metals on the magnetism of Fe in multilayers, because at the interface layer the two metals are expected to behave like a miscible alloy. We prepared multilayer films consisting of Fe and Zn metals (melting point of Zn is 692 K), which are immiscible, and investigated the relationships between magnetism and the structure as well as the thickness dependence of magnetism.

2. Experimental

Fe/Zn multilayers were prepared by alternate vapor deposition of pure Zn and Fe at a rate of 0.1–0.2 Å/s in an ultra-high-vacuum electron-beam evaporation system. The magnetic layer thickness t_{Fe} varied between 10 and 145 Å while the Zn layer t_{Zn} was kept constant at 20 Å. Samples were deposited on glass and kapton substrates at 300 K using a Zn buffer layer 100 Å thick. The Zn top layer in all samples was 50 Å thick. The growth parameters will be designated as $(t_{\text{Fe}}/t_{\text{Zn}})_n$, where n indicates the number of bilayers. X-ray diffraction ($\lambda_{\text{CuK}\alpha} = 1.542 \text{ \AA}$) was employed to analyze the periodicity and microstructure of the multilayers. Magnetization and $M-H$ loops were measured with a vibrating-sample magnetometer (VSM) under a maximum field of 1.5 T. FMR spectrum was obtained by a commercial electron paramagnetic spectrometer (EPR) operating at a frequency of 9.78 GHz with an applied field up to 1.7 T.

3. Results and discussion

Figs. 1 shows the low- and high-angle X-ray diffraction patterns for the $(\text{Fe } 15 \text{ \AA}/\text{Zn } 20 \text{ \AA})_{30}$ multilayer grown at 300 K on top of a 100 Å-thick Zn layer. Low-angle X-ray pattern (Fig. 1a) from the multilayer shows small Bragg peaks and the period deduced from the peak position agrees with the designed value, which confirms the periodically layered structure of the films.

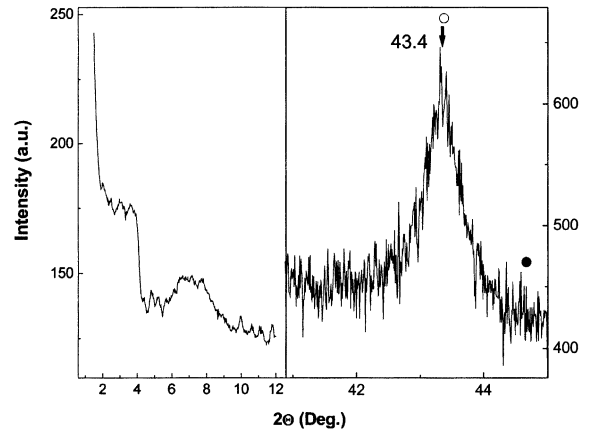


Fig. 1. The low-angle (a) and high-angle (b) X-ray diffraction patterns for a $(\text{Fe}15 \text{ \AA}/\text{Zn } 20 \text{ \AA})_{30}$ multilayer. The peak marked (○) corresponds to the disordered interface phase and the peak marked (●) corresponds to α -Fe.

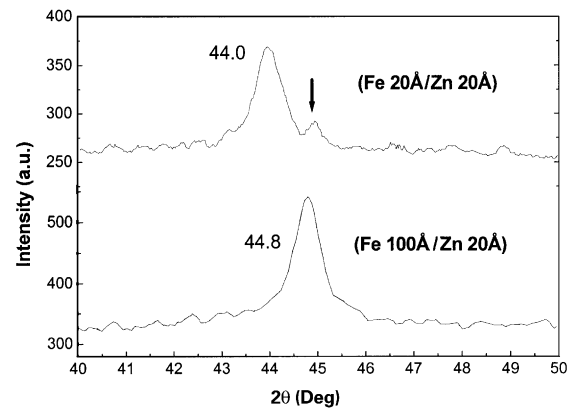


Fig. 2. High-angle X-ray diffraction patterns for $(\text{Fe } 20 \text{ \AA}/\text{Zn } 20 \text{ \AA})$ and $(\text{Fe } 100 \text{ \AA}/\text{Zn } 20 \text{ \AA})$ multilayers. The marked peak corresponds to α -Fe.

The high-angle X-ray diffraction pattern (Fig. 1b) shows a broadened line typical of a noncrystalline compound. This broadening could be a signature of a disordered Fe layer or a mixture of the Fe–Zn layers with a varied composition. The X-ray diffraction does not allow us to conclude on the structure of the interface. Fig. 2 shows the X-ray diffraction for $t_{\text{Fe}} > 20 \text{ \AA}$, additional peaks, characteristic of the α -iron phase, appear due to pure iron in the center of the iron layers.

Fig. 3 shows the Fe layer thickness dependence of the saturation magnetization per Fe volume for the Fe/Zn multilayer films. The values for the film with t_{Fe} more than 20 Å thick is in fairly good agreement with the bulk. However, the magnetization decreases with decreasing Fe layer thickness for values below 20 Å. Our results would indicate

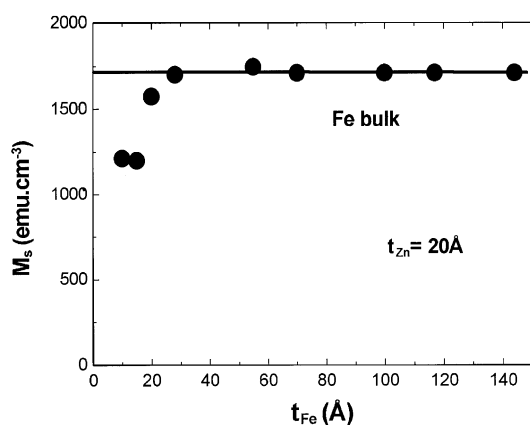


Fig. 3. The t_{Fe} dependence of the magnetization at 300 K.

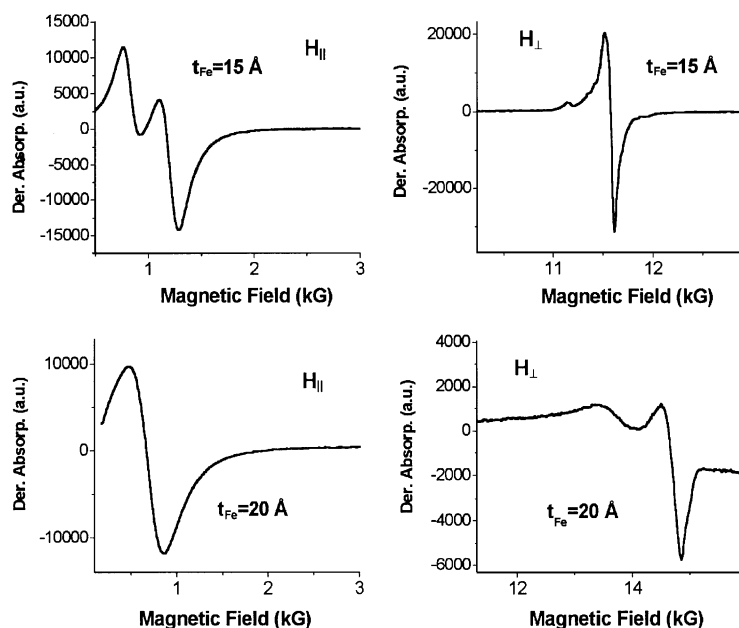


Fig. 4. FMR spectra for Fe 15 Å/Zn 20 Å and Fe 20 Å/Zn 20 Å multilayers. (\parallel) Applied DC field along the film plane, and (\perp) applied DC perpendicular to the plane at 300 K.

that the interface is diffused due to mixing effects, which is not surprising considering the low melting point of Zn.

In the FMR spectra, the absorption line with maximum intensity is the uniform mode, corresponding to the regular in-phase excitation of the magnetization in the Fe/Zn multilayers. Fig. 4 shows some typical derivative spectra of FMR for two samples (Fe 15 Å/Zn 20 Å) and (Fe 20 Å/Zn 20 Å). The symbols \parallel and \perp on the curves indicate that the applied magnetic field H is parallel or perpendicular to the film plane, respectively. The FMR spectra for H_{\parallel} for all the samples show a single absorption mode except for $t_{\text{Fe}} = 15$ Å.

For $t_{\text{Fe}} = 15$ Å, besides the uniform mode, there are some absorption lines in the FMR spectra. For such a film, the Fe layers may not be ideally continuous and also may have some mixing with the Zn layers. Thus the effective field is not completely homogeneous throughout the entire Fe layer.

The experimental results show that ΔH_{\parallel} decreases with increasing Fe thickness t_{Fe} : $\Delta H_{\parallel} = 642$ G for $t_{\text{Fe}} = 10$ Å and $\Delta H_{\parallel} = 160$ G

Table 1
Summary of magnetic parameters of Fe/Zn multilayers

t_{Fe} (Å)	$4\pi M_{\text{eff}}$ (G)	ΔH_{\parallel} (G)
10	6894	642
15	8225	198
20	10840	321
28	11000	170
55	15431	160
70	15910	170
100	16958	170
117	18130	302
144	18129	293

for $t_{\text{Fe}} = 55 \text{ \AA}$ (Table 1). The linewidth of the multilayer is attributed to a distribution of shape anisotropies.

The general expression of FMR condition for the uniform precession mode, valid for all magnitudes and directions of the applied field is given by [10]

$$(\omega/\gamma)^2 = (1/M_S^2)[F_{\theta\theta}(F_{\phi\phi}/\sin^2\theta + \cos\theta F_{\theta}/\sin\theta) - (F_{\theta\phi}/\sin\theta - \cos\theta F_{\phi}/\sin^2\theta)^2], \quad (1)$$

where $\omega = 2\pi f$ ($f = 9.78 \text{ GHz}$) is the microwave angular frequency, $\gamma = ge/2mc$ is the gyromagnetic ratio, g is the g -factor for the multilayers and M_S is the saturation magnetization. F_{ϕ} , $F_{\theta\phi}$ are the first and second derivatives of the total free energy density F with respect to the azimuthal ϕ and the polar angle θ of the magnetization relative to the z -axis directed along the film normal.

For the film that is isotropic in the film plane but having a uniaxial anisotropy along the film normal, it seems reasonable to express the free energy in the form: $F = -\mathbf{M} \cdot \mathbf{H} + (K_1 - 2\pi M_S^2)\sin^2\theta + K_2 \sin^4\theta$, where K_1 and K_2 are the lowest order anisotropy constants, the constant K_2 is at least one order smaller than K_1 [11]. The direction of the external DC magnetic field \mathbf{H} is defined by the polar angle θ_H and the azimuthal angle ϕ_H .

The resonance condition derived from Eq. (1) is given by

$$(\omega/\gamma)^2 = [H_r \cos(\theta - \theta_H) - 4\pi M_{\text{eff}} \cos^2\theta + (K_2/M_S)\sin^2 2\theta] \times [H_r \cos(\theta - \theta_H) - 4\pi M_{\text{eff}} \cos 2\theta + (4K_2/M_S) \times (\sin^2 2\theta - \sin^2\theta)]. \quad (2)$$

According to the equilibrium equations of the magnetization M_S , we have the following equation:

$$M_S H \sin(\theta - \theta_H) + (K_1 = 2\pi M_S^2) \sin 2\theta + 4K_2 \sin^3\theta \cos\theta = 0, \quad (3)$$

where

$$\begin{aligned} 4\pi M_{\text{eff}} &= 4\pi M_S - 2K_1/M_S \\ &= -(2/M_S)(K_1 - 2\pi M_S^2) \\ &= -2K_{\text{eff}}/M_S. \end{aligned}$$

M_{eff} and K_{eff} are the effective magnetization and the effective magnetic anisotropy constant, respectively.

According to Eqs. (2) and (3), in perpendicular geometry ($\theta_H = 0$), $\theta = 0$, $H_r = H_{\perp}$,

$$(\omega/\gamma)_{\perp} = H_{\perp} - 4\pi M_{\text{eff}} \quad (4)$$

and in parallel geometry ($\theta_H = 90^\circ$), $\theta = 90^\circ$, $H_r = H_{\parallel}$,

$$(\omega/\gamma)_{\parallel}^2 = H_{\parallel}(H_{\parallel} + 4\pi M_{\text{eff}}). \quad (5)$$

Knowing the resonance field H_{\perp} and H_{\parallel} in the perpendicular and parallel geometries, $4\pi M_{\text{eff}}$, K_{eff} , K_1 , and γ can be obtained according to Eqs. (4) and (5). The value of g was found to be quite close to the one previously reported [12], $g = 2.1$.

It is well known that the layer thickness dependence of the anisotropy in multilayers can be described, based on the phenomenological model, by the equation $K_{\text{eff}} = K_V + 2K_S/t_{\text{Fe}}$, where K_{eff} is the measured anisotropy, and K_V , K_S are the volume and the interface anisotropy (the factor of two arises from the two interfaces of each sublayer, which are assumed to contribute in the same way). The term K_V consists of three contributions: (1) the demagnetizing energy $2\pi M_S^2$, (2) the intrinsic crystalline anisotropy K_{MC} , and (3) the magnetoelastic anisotropy K_{ME} , which arises from the interaction of magnetostriction λ with the stress in the film. This is given by the term $K_{\text{ME}} = -3/2\sigma\lambda$, where σ is the stress.

The product $K_{\text{eff}} \times t_{\text{Fe}}$ versus t_{Fe} at 300 K is plotted in Fig. 5 for the samples with $10 \leq t_{\text{Fe}} \leq 144 \text{ \AA}$. The anisotropy data show a linear thickness dependence, except for $t_{\text{Fe}} < 25 \text{ \AA}$ where

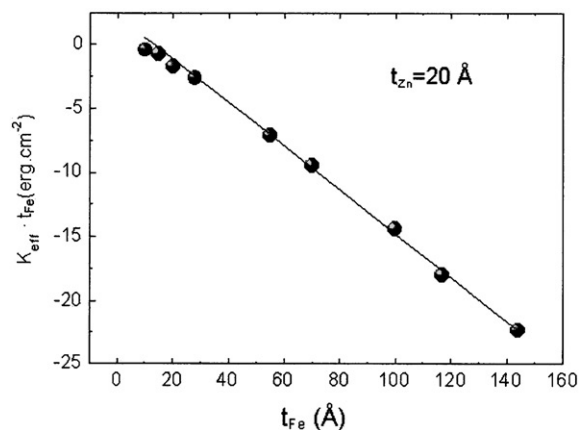


Fig. 5. The t_{Fe} dependence of the product $K_{eff} \times t_{Fe}$ at 300 K.

the values are below the straight line. One might understand this deviation as an indication for a tendency for island formation at low t_{Fe} due to bad wetting of Fe on Zn, which leads to smaller interface areas. However, there may be a transition (at a critical layer thickness t_{crit}) from an incoherent to a coherent structure in the presence of misfit strain anisotropy.

The experimental data are well described by a linear relation corresponding to $K_V = -1.7 \times 10^7$ erg/cm³ and $K_S = 1.0$ erg/cm². Here K_S is a positive value, which means that the interface anisotropy confines the magnetization to the direction of the film normal; this value is comparable with the one found in a very thin film iron [13]. K_S may contain Néel anisotropy [14] and misfit strain anisotropy from the incoherent lattice structure between adjacent layers in a multilayer [15,16].

The critical layer thickness t_{crit} can be expressed as follows [17]:

$$t_{crit} = 0.114 b \eta^{-1.22}, \quad (9)$$

where b is the Burgers vector and η is the lattice misfit. Taking $t_{crit} = 25$ Å, η can be about 0.025.

4. Conclusion

We have report studies on Fe/Zn multilayers prepared by evaporation in ultra-high vacuum.

The saturation magnetization for the Fe/Zn multilayer film decreases with Fe layer thickness for values below 20 Å. These results can be explained in terms of the interdiffusion between Fe and Zn atoms near the Fe–Zn interface. Simultaneously, the effective magnetization $4\pi M_{eff}$ and the resonance linewidth ΔH_{\parallel} are found to change correlatively with varying Fe layer thickness. This phenomenon can be explained as a result of the low-dimensional effect and the restricted distribution of shape anisotropies. The interface anisotropy is a positive value, which means that the interface anisotropy confines the magnetization to the direction of the film normal.

Acknowledgements

This work has been supported by CNPq and FAPERJ. H. Lassri thanks PCI/MCT program for the visitor fellowship and A.Y. Takeuchi for the support in the VSM measurements. M.A. Morales acknowledges CNPq for his doctor fellowship.

References

- [1] J.J. Krebs, P. Lubitz, A. Chaiken, G.A. Prinz, Phys. Rev. Lett. 63 (1989) 1645.
- [2] A. Cebollada, J.L. Martinez, J.M. Callego, J.J. de Miguel, R. Miranda, S. Ferrer, F. Batallan, G. Fillion, J.P. Rebouillat, Phys. Rev. B 39 (1989) 9726.
- [3] J.J. Rhyne, R.W. Erwin, J. Borchers, S. Sinha, M.B. Salamon, R. Dsu, C.P. Flynn, J. Appl. Phys. 61 (1987) 4043.
- [4] B. Heinrich, Z. Celinski, J.F. Cochran, W.B. Muir, J. Rudd, O.M. Zhong, A.S. Arrott, K. Myrtle, Phys. Rev. Lett. 64 (1990) 673.
- [5] N. Sato, IEEE Trans. Magn. 26 (1990) 2736.
- [6] Shigeki Nakagawa, Masahiko Naoe, J. Appl. Phys. 70(10) (1991) 6424.
- [7] Y. Ueda, A. Koizumi, K. Mukasa, J. Magn. Mater. 126 (1993) 28.
- [8] Y. Ueda, J. Appl. Phys. Jpn. 18 (1969) 1269.
- [9] R. Krishnan, H. Lassri, Solid State Commun. 84 (1992) 413.
- [10] L. Baselgia, M. Warden, F. Waldner, S.L. Hutton, J.E. Drumheller, Y.Q. He, P.E. Wigen, M. Marysko, Phys. Rev. B 38 (1988) 2237.

- [11] J. Ben Youssef, H. Le Gall, N. Vukadinovic, V. Gehanno, A. Marty, Y. Samson, B. Gilles, *J. Magn. Magn. Mater.* 202 (1999) 277.
- [12] H. Takahashi, K. Mitsuoka, M. Komuro, Y. Sugita, *J. Appl. Phys.* 73 (1993) 6060.
- [13] K.B. Urquhart, B. Heinrich, J.F. Cochran, A.S. Arrot, K. Myrtle, *J. Appl. Phys.* 64 (1998) 5334.
- [14] L. Néel, *J. Phys. Rad.* 15 (1954) 225.
- [15] F.J.A. den Broeder, W. Hoving, P.J.H. Bloemen, *J. Magn. Magn. Mater.* 93 (1991) 562.
- [16] F.J.A. den Broeder, D. Kuiper, A.P. Van de Mosselaer, W. Hoving, *Phys. Rev. Lett.* 60 (1988) 2769.
- [17] J.H. van der Merwe, W.A. Jesser, *J. Appl. Phys.* 63 (1988) 1509.